

# Superfluid Phase Transitions in Dense Neutron Matter

V. A. Khodel,<sup>1,2</sup> J. W. Clark,<sup>1</sup> and M. V. Zverev<sup>2</sup>

<sup>1</sup>*McDonnell Center for the Space Sciences and Department of Physics,*

*Washington University, St. Louis, MO 63130 USA*

<sup>2</sup>*Russian Research Center Kurchatov Institute, Moscow 123182, Russia*

(October 25, 2018, Submitted to Physical Review Letters)

## Abstract

The phase transitions in a realistic system with triplet pairing, dense neutron matter, have been investigated. The spectrum of phases of the  ${}^3P_2$ - ${}^3F_2$  model, which adequately describes pairing in this system, is analytically constructed with the aid of a separation method for solving BCS gap equations in states of arbitrary angular momentum. In addition to solutions involving a single value of the magnetic quantum number (and its negative), there exist ten real multicomponent solutions. Five of the corresponding angle-dependent order parameters have nodes, and five do not. In contrast to the case of superfluid  ${}^3\text{He}$ , transitions occur between phases with nodeless order parameters. The temperature dependence of the competition between the various phases is studied.

arXiv:nucl-th/0101045v1 20 Jan 2001

Superfluid systems manifesting triplet pairing between constituent spin-1/2 fermions are exemplified by liquid  $^3\text{He}$  at millikelvin temperatures and by the neutronic component of the quantum fluid interior of a neutron star. In the latter case, the density becomes high enough that the familiar singlet  $S$ -wave gap has closed and pairing in the  $^3P_2$  channel is favored by the spin-orbit force acting between neutrons [1–4]. The determination of superfluid phase diagrams for such systems over an extensive temperature range has presented a difficult challenge for theorists. On the one hand, the standard Ginzburg-Landau approach is valid only for temperatures near the critical temperature  $T_c$ . On the other hand, iterative procedures, commonly used to calculate the energy gap in systems with  $S$ -wave pairing, suffer from slow convergence and uncertain accuracy when applied to the many coupled nonlinear integral equations that arise for BCS pairing in higher angular momentum states.

Limitations of the standard iterative approaches are accentuated when one attempts to construct the superfluid phase diagram of the system, which is orchestrated by tiny energy splittings between the different solutions of the BCS pairing problem. This problem is ordinarily framed in terms of the set of equations [4]

$$\begin{aligned} \Delta_L^{JM}(p) = & \sum_{L'L_1J_1M_1} (-1)^{1+\frac{L-L'}{2}} \int \int \langle p | V_{LL'}^J | p_1 \rangle S_{L'L_1}^{JM J_1 M_1}(\mathbf{n}_1) \\ & \times \frac{\tanh(E(\mathbf{p}_1)/2T)}{2E(\mathbf{p}_1)} \Delta_{L_1}^{J_1 M_1}(p_1) p_1^2 dp_1 d\mathbf{n}_1 \end{aligned} \quad (1)$$

for the coupled partial-wave components that appear in the expansion

$\Delta_{\alpha\beta}(\mathbf{p}) = \sum_{J,L,M} \Delta_L^{JM}(p) \left( G_{LJ}^M(\mathbf{n}) \right)_{\alpha\beta}$  of the  $2 \times 2$  gap matrix in terms of the spin-angle matrices  $\left( G_{LJ}^M(\mathbf{n}) \right)_{\alpha\beta} = \sum_{M_S M_L} C_{\frac{1}{2}\frac{1}{2}\alpha\beta}^{1M_S} C_{1LM_S M_L}^{JM} Y_{LM_L}(\mathbf{n})$ . The quasiparticle energy

$$E(\mathbf{p}) = \left[ \xi^2(p) + \frac{1}{2} \sum_{LJM L_1 J_1 M_1} \left( \Delta_L^{JM}(p) \right)^* \Delta_{L_1}^{J_1 M_1}(p) S_{L L_1}^{JM J_1 M_1}(\mathbf{n}) \right]^{\frac{1}{2}}, \quad (2)$$

is constructed from the gap components  $\Delta_L^{JM}(p)$  together with the single-particle spectrum  $\xi(p) \simeq p_F(p - p_F)/M^*$  of the normal Fermi liquid, where  $M^*$  is a suitable effective mass. This quantity is rendered angle dependent by the spin trace  $S_{L L_1}^{JM J_1 M_1}(\mathbf{n}) = \text{Tr} \left[ \left( G_L^{JM}(\mathbf{n}) \right)^* G_{L_1}^{J_1 M_1}(\mathbf{n}) \right]$ , further complicating explicit solution of the system (1).

The pairing matrix elements  $\langle p|V_{LL'}^J|p_1\rangle$  are generated by the spin-angle expansion  $V(\mathbf{p}, \mathbf{p}_1) = \sum_{LL'JM} (-1)^{\frac{L-L'}{2}} \langle p|V_{LL'}^J|p_1\rangle G_{LJ}^M(\mathbf{n}) \left(G_{L'J}^M(\mathbf{n}_1)\right)^*$  of the block of Feynman diagrams irreducible in the particle-particle channel. A salient feature of the vacuum  $nn$  interaction is that the components of the central forces nearly compensate each other, as evidenced in the experimental  $P$ -scattering phases [5]. We shall assume that this feature is preserved by the effective  $nn$  interaction inside neutron matter. The dominant role of the spin-orbit component in promoting the  ${}^3P_2$  pairing channel at super-nuclear densities then implies that contributions to triplet pairing from nondiagonal terms with  $L', L_1 \neq 1$  or  $J_1 \neq 2$  on the r.h.s. of Eq. (1) can be evaluated within perturbation theory, in terms of the set of principal gap amplitudes  $\Delta_1^{2M}(p)$ , with  $M$  running from  $-2$  to  $2$ . In fact, time-reversal invariance implies that the problem may be treated in terms of only three complex functions, namely  $\Delta_1^{2M}(p)$  with  $M = 0, 1, 2$ .

Essential further simplifications are possible if we apply the separation approach developed in [6], which establishes the factorization

$$\Delta_1^{2M}(p) = D_1^{2M} \chi(p), \quad M = 0, 1, 2, \quad (3)$$

where  $\chi(p)$  is a universal shape factor normalized to unity at  $p = p_F$ . As a consequence, the elucidation of the phase diagram of dense superfluid neutron matter reduces to the determination of the three coefficients  $D_1^{2M}$ , since the character of the phase diagram itself is independent of the shape factor  $\chi(p)$ .

Among the nondiagonal contributions to the r.h.s. of Eq. (1), two assume leading importance. The first contains the integral of the product  $V_{31}^2 S_{31}^{2M2M_1} \Delta_1^{2M_1}$ , while the second contains the integral of the product  $V_{11}^2 S_{13}^{2M2M_1} \Delta_3^{2M_1}$ . Considering only these contributions, we obtain the  ${}^3P_2$ - ${}^3F_2$  pairing problem, which has been treated numerically in earlier work, notably Refs. [3,4,7,8]. The list of relevant states appears to be exhausted with the addition of the (less important)  ${}^3P_0$  and  ${}^3P_1$  pairing channels [8]. The rapid convergence of the nondiagonal integrals on the r.h.s. of the gap equations (1) greatly facilitates implementation of the perturbation strategy, since the overwhelming contributions to these integrals come

from the region adjacent to the Fermi surface. For  $E(\mathbf{p})$  significantly in excess of the energy gap value  $\Delta_F$ , the energies  $E(\mathbf{p})$  and  $|\xi(p)|$  practically coincide and, as a result, the angular integration yields zero. Thus, when dealing with the nondiagonal contributions, it is sufficient to know the minor gap components  $\Delta_3^{2M}(p)$  (with  $M = 0, 1, 2$ ) at the point  $p = p_F$ , which may be efficiently evaluated in terms of the coefficients  $D_1^{2M}$  with the aid of the set (1) itself. In doing so, we retain on the r.h.s. of (1) only the dominant contribution containing a large logarithmic factor  $\ln(\epsilon_F/\Delta_F)$ , where  $\epsilon_F$  is the Fermi energy. This leads to the simple connection

$$\Delta_3^{2M}(p = p_F) = \eta D_1^{2M} , \quad (4)$$

where  $\eta = -\langle p_F | V_{13}^2 | p_F \rangle / v_F$  and  $v_F \equiv \langle p_F | V_{11}^2 | p_F \rangle$ . Analogous linear relations hold for other minor components  $\Delta_L^{JM}$  of the gap function (notably  $\Delta_1^{00}$  and  $\Delta_1^{1M}$ ).

When calculated for in-vacuum neutron-neutron interactions [9], the  $\eta$  value depends smoothly on  $\rho$ , varying around 0.3 in the interval  $\rho_0 < \rho < 3\rho_0$  [8]. In view of its relativistic origin, the spin-orbit force should not be much affected by polarization or correlation corrections, a judgment supported by the empirical analysis of spin-orbit splitting in finite nuclei. Medium modification of the tensor force may be more significant, especially in the environs of the pion-condensation phase transition [10,11]. Investigation of this possibility calls for special treatment and will be pursued elsewhere.

A complete understanding of the phase diagram of systems that exhibit triplet pairing would require the inclusion of corrections to the in-medium interaction depending on the pairing gap itself. These “strong-coupling” corrections are most important near the critical temperature  $T_c$  [12,13]. Their effect is not addressed in the present work, which focuses on temperatures far enough below  $T_c$  that pairing corrections to the vertex  $V$  (and hence to the parameter  $\eta$ ) may be ignored.

We turn now to the determination of the key coefficients  $D_1^{2M}$  ( $M = 0, 1, 2$ ) to leading perturbative order in the parameter  $\eta$ . Making use of the connection (4), simple manipulations of Eqs. (1) at  $p = p_F$  yield three coupled equations for these coefficients,

$$D_1^{2M} + v_F \sum_{M_1} D_1^{2M} \int \int \phi(p) \frac{\tanh(E_0(\mathbf{p})/2T)}{2E_0(\mathbf{p})} S_{11}^{2M_2M_1}(\mathbf{n}) \chi(p) p^2 dp d\mathbf{n} = \eta v_F r_M, \quad (5)$$

with  $\phi(p) \equiv \langle p | V_{11}^2 | p_F \rangle / v_F$ ,  $E_0(\mathbf{p}) \equiv E(\mathbf{p}; \eta = 0)$ , and

$$r_M = \sum_{M_1} D_1^{2M_1} \int \int [S_{31}^{2M_2M_1}(\mathbf{n}) + S_{13}^{2M_2M_1}(\mathbf{n})] \frac{\tanh(E_0(\mathbf{p})/2T)}{2E_0(\mathbf{p})} p^2 dp d\mathbf{n}. \quad (6)$$

The search for solutions will be confined to those with real coefficients  $D_1^{2M}$  since, as a rule, such states lie lower in energy than those with complex  $D_1^{2M}$ . Inserting the explicit form of  $S_{11}^{2M_2M_1}(\mathbf{n})$  into Eqs. (5) and (6), we may arrive at a system of three equations

$$\begin{aligned} \lambda_2 + v_F [\lambda_2(J_0 + J_5) - \lambda_1 J_1 - J_3] &= \eta v_F r_2, \\ \lambda_1 + v_F [-(\lambda_2 + 1)J_1 + \lambda_1(J_0 + 4J_5 + 2J_3)/4] &= \eta v_F r_1, \\ 1 + v_F [-(\lambda_2 J_3 + \lambda_1 J_1)/3 + J_5] &= \eta v_F r_0, \end{aligned} \quad (7)$$

for the two ratios  $\lambda_1 = D_1^{21}/D_1^{20}\sqrt{6}$  and  $\lambda_2 = D_1^{22}/D_1^{20}\sqrt{6}$  and the gap value  $\Delta_F$ . These equations are written so as to coincide at  $\eta = 0$  with the equations of the pure  ${}^3P_2$  pairing model solved in Ref. [8], where

$$J_i = \int \int f_i(\theta, \varphi) \phi(p) \frac{\tanh E_0(\mathbf{p})/2T}{2E_0(\mathbf{p})} \chi(p) \frac{p^2 dp d\mathbf{n}}{4\pi} \quad (8)$$

with  $f_0 = 1 - 3z^2$ ,  $f_1 = 3xz/2$ ,  $f_3 = 3(2x^2 + z^2 - 1)/2$ , and  $f_5 = (1 + 3z^2)/2$  and  $z = \cos \theta$ ,  $x = \sin \theta \cos \phi$ , and  $y = \sin \theta \sin \phi$ . Of the integrals  $J_i$  (with  $j = 1, \dots, 5$ ), only  $J_5$  contains a principal term going like  $\ln(\epsilon_F/\Delta_F)$ .

Eqs. (7) have three familiar *one-component* solutions [2,4,8] corresponding to  $M = 0, 1$ , and 2. To establish the structure and the spectrum of the *multicomponent* solutions of the perturbed problem, we carry out a two-step transformation of the set (7). The integral  $J_5$  is responsible for introducing the gap value  $\Delta_F$  but is irrelevant to the phase structure. Thus, as a first step we combine the equations (7) so as to eliminate terms involving  $J_5$  from the first pair and, in addition, reduce the number of the  $J_i$  integrals in each equation to two. The resulting  $J_5$ -independent equations are

$$\begin{aligned} (\lambda_2 + 1)[3\lambda_1(\lambda_2 + 1)J_0 - 2(\lambda_1^2 - 2\lambda_2^2 + 6)J_1] &= \eta B_1, \\ (\lambda_2 + 1)[(\lambda_1^2 - 4\lambda_2)J_1 + \lambda_1(\lambda_2 + 1)J_3] &= \eta B_2, \end{aligned} \quad (9)$$

where  $B_1 = 2\lambda_1(2\lambda_2+3)r_2 - 4(\lambda_2^2-3)r_1 - 6\lambda_1(\lambda_2+2)r_0$  and  $B_2 = -\lambda_1r_2 + 4\lambda_2r_1 - 3\lambda_1\lambda_2r_0$ . The second step is taken under the assumption that  $\lambda_2 \neq 1$ ; otherwise the ensuing manipulations lose their meaning. As in Ref. [6], we perform the rotation  $(x, z) = (-t \sin \vartheta + u \cos \vartheta, t \cos \vartheta + u \sin \vartheta)$ , choosing the angle  $\vartheta$  to remove the integral  $J_1$  from Eqs. (9). In particular, if  $\zeta = \tan \vartheta$  is chosen to obey the algebraic equation  $\lambda_1\zeta^2 - (\lambda_2 - 3)\zeta - \lambda_1 = 0$ , substitution of the transformed integrals  $J_i$  into Eqs. (9) yields

$$\begin{aligned}(\lambda_2 + 1)[A_1J_0 + A_2J_3] &= \eta B_1 , \\(\lambda_2 + 1)[A_1J_0 + A_2J_3] &= -2\eta B_2 ,\end{aligned}\tag{10}$$

with  $A_1 = \frac{3}{2}\lambda_1(1 + \lambda_2)(2 - \zeta^2) - \frac{3}{2}(\lambda_1^2 - 2\lambda_2^2 + 6)\zeta$  and  $A_2 = -3\lambda_1(1 + \lambda_2)\zeta^2 - (\lambda_1^2 - 2\lambda_2^2 + 6)\zeta$ .

We observe that the left-hand members of these two equations (12) are identical. It is just this feature that leads to the universalities of the pure  ${}^3P_2$  pairing problem discovered in Ref. [6]. Independently of temperature, density, and details of the in-medium interaction, the solutions of this restricted problem derived from Eqs. (9) at  $\eta \equiv 0$  (where the right-hand members of Eqs. (12) are trivially coincident) fall into two groups degenerate in energy, namely an upper group comprised of states whose angle-dependent order parameters have nodes and a lower group with nodeless order parameters (cf. Ref. [14]). In addition to the energy degeneracies, the multicomponent pairing solutions, which satisfy

$$(\lambda_1^2 + 2 - 2\lambda_2)(\lambda_1^2 - 2\lambda_2^2 - 6\lambda_2) = 0 ,\tag{11}$$

display a degeneracy with respect to the coefficient ratios  $\lambda_1$  and  $\lambda_2$ , since they generally define *curves* rather than *points* in the  $(\lambda_1, \lambda_2)$  plane.

The strong parametric degeneracy inherent in pure  ${}^3P_2$  pairing is lifted in the case of  ${}^3P_2$ - ${}^3F_2$  pairing: at  $\eta > 0$  the true solutions of the problem are represented by a set of isolated points in the  $(\lambda_1, \lambda_2)$  plane. Indeed, upon equating the right-hand members of Eqs. (10) in the small- $\eta$  limit, one obtains an additional relation between the parameters  $\lambda_1(\eta = 0)$  and  $\lambda_2(\eta = 0)$ , viz.

$$\lambda_1r_2 - (\lambda_2 - 3)r_1 - 3\lambda_1r_0 = 0 ,\tag{12}$$

where the  $r_M$  are defined by Eq. (6). This relation supplements the spectral condition (11) and lifts the parametric degeneracy.

The system formed by (11) and (12) is solved analytically by utilizing the same rotation in  $x - z$  coordinates as described above. After lengthy algebra, one arrives at the full set of solutions of the coupled-channel  ${}^3P_2$ - ${}^3F_2$  pairing problem. A conspicuous feature of these solutions, made transparent by the separation method [6], is their virtually complete independence of the temperature  $T$ .

Before cataloging and classifying the  ${}^3P_2$ - ${}^3F_2$  pairing solutions, it is worth pointing out that the particular solution  $\lambda_2 = -1$  found in the pure  ${}^3P_2$  problem remains intact upon switching on the  ${}^3F_2$  channel, but it completely disappears if any further channel (e.g.  ${}^3P_0$ ) enters the picture.

Fig. 1 summarizes the results of our analytical considerations. Only the right half of the  $(\lambda_1, \lambda_2)$  plane is shown, since the relevant energies are independent of the sign of  $\lambda_1$ . Besides the well-known single-component solutions with  $|M| = 0, 1, \text{ or } 2$ , the collection of unitary solutions of the  ${}^3P_2$ - ${}^3F_2$  pairing problem contains *ten* multicomponent solutions, corresponding to more complicated superfluid phases. *Five* of these additional solutions, denoted  $O_k$  ( $k = 1, \dots, 5$ ), have nodeless order parameters and include:

- (a) *Two* two-component solutions  $O_{\pm 3}$ , identical to those found in the pure  ${}^3P_2$  pairing problem, with  $\lambda_1 = 0$  and  $\lambda_2 = \pm 3$ .
- (b) *Three* three-component solutions, two of which,  $O_1$  and  $O_4$ , are associated with the upper branch of  $\lambda_1^2 - 2\lambda_2^2 - 6\lambda_2 = 0$  and have  $\lambda_2 = 3(\sqrt{21}-4)/5$  and  $\lambda_2 = 3$ , respectively; while a third,  $O_2$ , is associated with the lower branch of the same equation and has  $\lambda_2 = -3(\sqrt{21}+4)/5$ .

The remaining five solutions of the problem, denoted by  $X_k$  ( $k = 1, \dots, 5$ ), are distinguished by order parameters that do have zeros. This set includes:

- (a) *Two* two-component solutions  $X_{\pm 1}$ , again identical to those found in the pure  ${}^3P_2$  pairing problem, with  $\lambda_1 = 0$  and  $\lambda_2 = \pm 1$ .

- (b) *Three* three-component solutions,  $X_2$ ,  $X_3$ , and  $X_4$ , associated with the parabola  $\lambda_2 = \lambda_1^2/2 + 1$  and having  $\lambda_2 = 13 - 2\sqrt{35}$ ,  $\lambda_2 = 3$ , and  $\lambda_2 = 13 + 2\sqrt{35}$ , respectively.

These general features of the spectrum of solutions of the  ${}^3P_2$ - ${}^3F_2$  problem are expected to persist even if  $\eta$  is not so small.

To construct the phase diagram of superfluid neutron matter, the third of Eqs. (7) must be brought into play to determine the gap values  $\Delta_F$  for the different solutions. We must then compare the free-energy shifts  $F_s = -\int \Delta_F^2(g)g^{-2}dg$  due to pairing in the corresponding superfluid states, where  $g$  is the relevant pairing coupling constant.

At low  $T$ , the only true contestants for existence and ascendancy are the solutions with nodeless order parameters, since the other solutions lie too high in energy; the gap between the states of the two different groups cannot be bridged if the value of  $|\eta|$  stays rather small. Thus, even though the degeneracy of the  ${}^3P_2$  pairing problem in the  $\lambda_1 - \lambda_2$  plane, embodied in the relation (11), is entirely removed when the  ${}^3P_2$ - ${}^3F_2$  coupling is switched on, the degeneracies in the energetic spectrum of the different superfluid phases are only partially lifted. Instead, this spectrum decays into several groups of nearly degenerate states, the  $O_1$  and  $O_2$  phases forming the lowest-energy group, the next higher group being composed of the phases  $O_{\pm 3}$  along with the one-component phase with  $M = 0$ , and so on. As seen in Fig. 2, the splitting between the two groups lowest in energy shrinks as  $T$  increases, until, at  $T \simeq 0.7T_c$ , their roles are interchanged and transitions occur. However, unlike the A-B phase transition in superfluid  ${}^3\text{He}$ , where the order parameter of the A-phase solution has nodes while that of the B-phase does not, the transition in neutron matter takes place between phases with nodeless order parameters. Introduction of the  ${}^3P_0$  and  ${}^3P_1$  pairing channels produces a further lifting of energy degeneracies and hence a further complication of the phase diagram of superfluid neutron matter. Unfortunately, it is not possible to resolve the resulting fine structure of the phase spectrum without more detailed information on the in-medium effective interaction between neutrons, which is currently unavailable.

The temperature region near  $T_c$  provides another venue for possible superfluid phase



transitions. In this regime, strong-coupling corrections should no longer be ignored [13], and the character of the phase diagram may be influenced significantly by external magnetic fields. Finally, fermion condensation, occurring as a precursor to pion condensation [15], should be mentioned as a source of exotic phase transitions in superfluid neutron matter at densities approaching the critical value for collapse of the pion mode [10].

If, as we have shown, the phase diagram of dense neutron matter exhibits several triplet superfluid phases, then phase transitions between different phases are expected to occur as the neutron star cools. Since the gap value changes in these transitions, their occurrence may ultimately be detected in the thermal history and/or the rotational dynamics of the star, for example in variation of its moment of inertia or in alterations of the distribution of the angular momentum between the crust and the vortex system, resulting in a change of the star's angular velocity. Possible scenarios leading to distinctive observable manifestations will be presented separately.

We thank A. D. Sedrakian, I. I. Strakovsky, G. E. Volovik, and D. N. Voskresensky for illuminating discussions. This research was supported in part by the U. S. National Science Foundation under Grant No. PHY-9900713 (JWC and VAK), by the McDonnell Center for the Space Sciences (VAK), and by Grant No. 00-15-96590 from the Russian Foundation for Basic Research (VAK and MVZ). MVZ acknowledges the hospitality of the INFN (Sezione di Catania).

## REFERENCES

- [1] M. Hoffberg, A. E. Glassgold, R. W. Richardson, M. Ruderman, Phys. Rev. Lett. **24**, 775 (1970).
- [2] T. Takatsuka and R. Tamagaki, Prog. Theor. Phys. **46**, 114 (1971).
- [3] T. Takatsuka, Prog. Theor. Phys. **48**, 1517 (1972).
- [4] L. Amundsen and E. Østgaard, Nucl. Phys. **A442**, 163 (1985).
- [5] R. A. Arndt, C. H. Oh, I. I. Strakovsky, R. L. Workman, and F. Dohrmann, Phys. Rev. C **56**, 3005 (1997).
- [6] V. A. Khodel, V. V. Khodel, and J. W. Clark, Phys. Rev. Lett. **81**, 3828 (1998).
- [7] M. Baldo, Ø. Elgarøy, L. Engvik, M. Hjorth-Jensen, and H.-J. Schulze, Phys. Rev. C **58**, 1921 (1998).
- [8] V. V. Khodel, V. A. Khodel, and J. W. Clark, Nucl. Phys. **A679**, 827 (2001).
- [9] R. B. Wiringa, V. G. J. Stoks, and R. Schiavilla, Phys. Rev. C **51**, 38 (1995).
- [10] A. B. Migdal, Rev. Mod. Phys. **50**, 107 (1978).
- [11] A. Akmal, V. R. Pandharipande, and D. G. Ravenhall, Phys. Rev. C **58**, 1804 (1998).
- [12] D. Vollhardt and P. Wölfle, *The Superfluid Phases of Helium 3* (Taylor & Francis, London, 1990).
- [13] J. A. Sauls, and J. W. Serene, Phys. Rev. D **17**, 1524 (1978).
- [14] R. W. Richardson, Phys. Rev. D **5**, 1883 (1972).
- [15] D. N. Voskresensky, V. A. Khodel, M. V. Zverev, and J. W. Clark, Ap. J. **533**, L127 (2000).

## Figure Captions

**Fig. 1.** Multicomponent solutions of the  ${}^3P_2$ - ${}^3F_2$  pairing problem. Solutions whose order parameter is nodeless [exhibit nodes] in the case of pure  ${}^3P_2$  pairing are indicated by filled [open] circles.

**Fig. 2.** Difference  $\delta\Delta_F^2(T)$  between the  $\Delta_F^2(T)$  values for the phases  $O_1$  or  $O_2$  and for the phases  $O_{\pm 3}$  (or the one-component phase with  $M = 0$ ), measured in units of  $|\delta\Delta_F^2(T = 0)|$ .

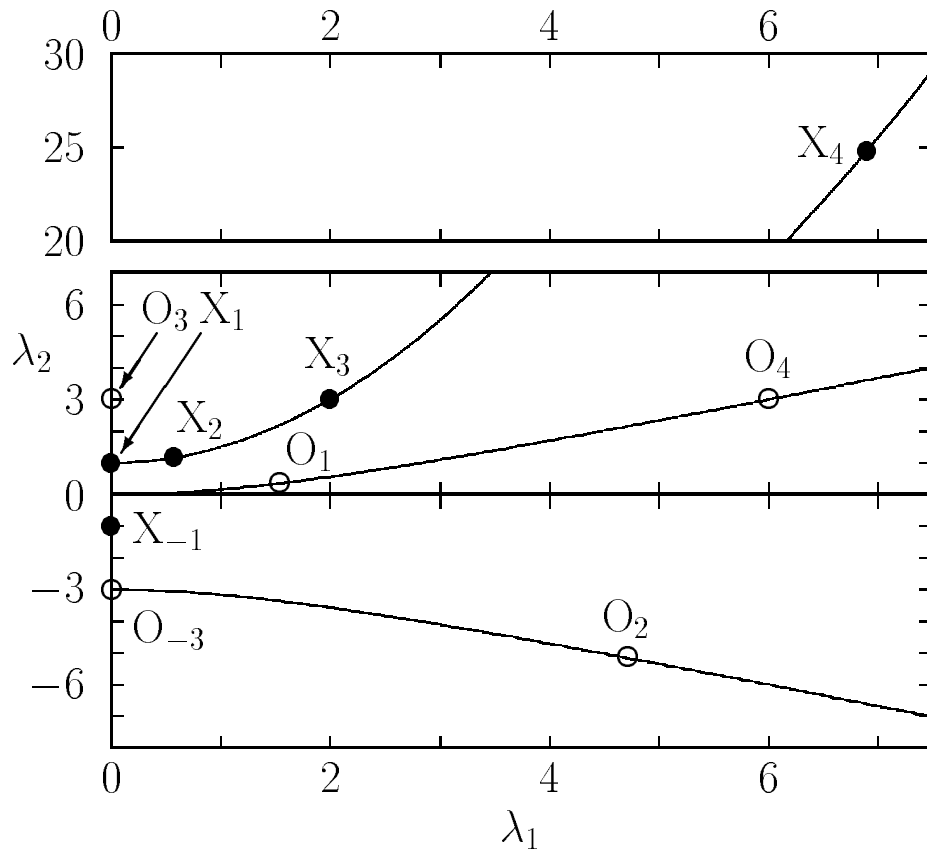
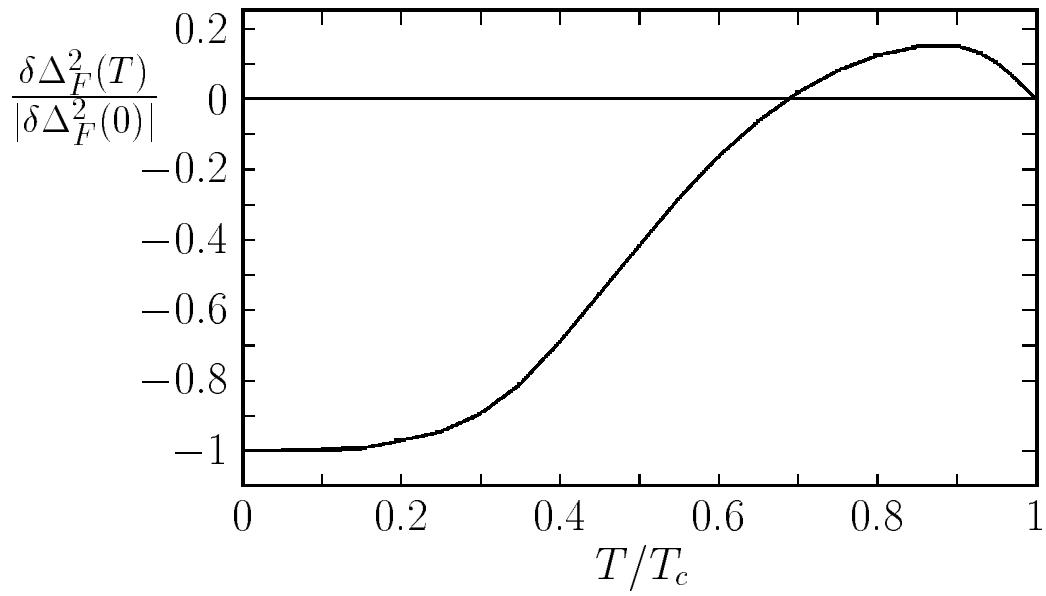


Fig. 1



**Fig. 2**